

# Recent progress in high temperature permanent magnetic materials

Cheng-Bao Jiang\*, Shi-Zhong An

Received: 4 September 2013 / Revised: 30 September 2013 / Accepted: 1 October 2013 / Published online: 30 October 2013  
© The Nonferrous Metals Society of China and Springer-Verlag Berlin Heidelberg 2013

**Abstract** Permanent magnetic materials capable of operating at high temperature up to 500 °C have wide potential applications in fields such as aeronautics, space, and electronic cars. SmCo alloys are candidates for high temperature applications, since they have large magnetocrystalline anisotropy field (6–30 T), high Curie temperature (720–920 °C), and large energy product ( $>200 \text{ kJ}\cdot\text{m}^{-3}$ ) at room temperature. However, the highest service temperature of commercial 2:17 type SmCo magnets is only 300 °C, and many efforts have been devoted to develop novel high temperature permanent magnets. This review focuses on the development of three kinds of SmCo based magnets: 2:17 type SmCo magnets, nanocrystalline SmCo magnets, and nanocomposite SmCo magnets. The oxidation protection, including alloying and surface modification, of high temperature permanent magnets is discussed as well.

**Keywords** Magnetic materials; Sm-Co alloys; Permanent magnets; High temperature

## 1 Introduction

During most of the twentieth century, the energy product of permanent magnets doubled every decade or two (Fig. 1), starting from  $\sim 10 \text{ kJ}\cdot\text{m}^{-3}$  for steels discovered in the early part of the century, increasing to  $\sim 450 \text{ kJ}\cdot\text{m}^{-3}$  for NdFeB magnets in the 1990s [1–3]. The rapid development of permanent magnets began in 1951, when the ferrimagnetic

hexagonal ferrites were discovered, which broke the shape barrier of magnets, and henceforth, the magnets could be made in any desired shape [3]. The 1960s brought the first generation of rare earth magnets—SmCo<sub>5</sub> magnets, then Sm<sub>2</sub>Co<sub>17</sub> magnets with an energy product of more than  $250 \text{ kJ}\cdot\text{m}^{-3}$  were developed. And in the 1980s, researchers devised NdFeB magnets, whose energy product eventually reaches about  $470 \text{ kJ}\cdot\text{m}^{-3}$ . But since 1990s, the energy product seems stalled, and no big breakthrough is insight during the past 20 years.

During the “stalled years” of magnets operating at ambient temperature since 1990s, permanent magnets capable of operating at high temperature up to 500 °C, so called high temperature permanent magnets, have attracted much interest due to their potential applications in fields such as aeronautics, space, and electronic cars [2, 4–6]. For instance, high temperature permanent magnets are required in gyroscopes, reaction and momentum wheels to control and stabilize satellites, and magnetic bearings [5]. For permanent magnets, the ability to resist demagnetization is characterized by coercivity  $H_c$ , which is extremely important for application in motor, etc., since the thermal demagnetization and field demagnetization occur simultaneously when the motor is running [2]. The  $H_c$  of permanent magnets should be high enough to maintain a linear  $B$ – $H$  curve which is a very important characteristic that enable the magnets to be stable during operation. Figure 2 shows the demagnetization curves for four major permanent magnets. The Alnico magnets have a high Curie temperature of more than 800 °C, but their coercivity is very low, and the  $B$ – $H$  curve is not linear. Only three types of permanent magnets in Fig. 2 possess a linear  $B$ – $H$  curve: ferrites, NdFeB, and SmCo magnets. NdFeB magnets have the largest energy product at room temperature, but their Curie temperature is  $\sim 312$  °C, and thus even if partially

C.-B. Jiang\*, S.-Z. An  
School of Materials Science and Engineering,  
Beihang University, Beijing 100191, China  
e-mail: jiangcb@buaa.edu.cn

substituting Dy for Nd can enhance the anisotropy field, the operation temperature of the magnets usually cannot exceed 200 °C. Ferrites have a positive temperature coefficient of coercivity which makes them a relatively good material for motor application up to 300 °C [2], but their Curie temperature is  $\sim 450$  °C, making them not suitable for application at 500 °C and above. Besides, the energy product of ferrites is relatively low ( $<40$  kJ·m<sup>-3</sup>). SmCo magnets have a large magnetocrystalline anisotropy field of 4,800–24,000 kA·m<sup>-1</sup>, a high Curie temperature of 720–920 °C, and an energy product of more than 200 kJ·m<sup>-3</sup> at room temperature, which makes them candidates for high temperature applications.

However, the highest service temperature of commercial 2:17 type SmCo magnets is only 300 °C, since their coercivity decreases sharply at higher temperature. In recent years, many efforts have been devoted to develop high temperature permanent magnets with high performance and researches are mainly focused on three types of magnets: 2:17 type SmCo magnets, nanocrystalline SmCo

magnets, and nanocomposite SmCo magnets. At the same time, the oxidation protection is an important issue for high temperature applications, and there have been substantial researches about it. This article presents an overview of recent research developments on high temperature permanent magnets, including the development of 2:17 type SmCo magnets, nanocrystalline SmCo magnets, nanocomposite SmCo magnets, and the oxidation protection of the magnets.

## 2 High temperature permanent magnets

### 2.1 2:17 type SmCo magnets

The traditional 2:17 type SmCo magnets can only service at less than 300 °C due to the large temperature coefficient of coercivity, which means the coercivity decreases rapidly with temperature increasing. 2:17 type SmCo high temperature permanent magnets with low coercivity temperature coefficient developed from the traditional 2:17 type SmCo magnets by adjusting the technical parameters such as composition and heat treatment. And further analysis shows that the low coercivity temperature coefficient is attributed to the modification of microstructure, microchemistry, and domain structure.

#### 2.1.1 Technical parameters

The novel 2:17 type SmCo alloys for high temperature applications is also Sm(CoFeCuZr)<sub>z</sub> ( $z = 6.0$ – $9.0$ ) quinary alloys like the traditional 2:17 type SmCo alloys. The main difference in composition is the Sm and Fe contents. In 1999, Liu et al. [7] reported a magnet with the nominal composition Sm(Co<sub>bal</sub>Fe<sub>0.1</sub>Cu<sub>0.078</sub>Zr<sub>0.033</sub>)<sub>8.3</sub>, which has a saturation magnetization  $M_s$  of 92 A·m<sup>2</sup>·kg<sup>-1</sup>, a room temperature intrinsic coercivity  $iH_c$  of 3,185 kA·m<sup>-1</sup>, a temperature coefficient of intrinsic coercivity of  $-0.15$  %·°C<sup>-1</sup> and a high intrinsic coercivity of 852 kA·m<sup>-1</sup> at 500 °C. With the increase of Fe content  $x$  from 0 to 0.25, the room temperature magnetic properties  $M_s$  and  $M_r$  of Sm(Co<sub>bal</sub>Fe<sub>x</sub>Cu<sub>0.078</sub>Zr<sub>0.033</sub>)<sub>8.3</sub> magnets increase monotonously, while the  $H_c$  first increases, peaks at  $x = 0.10$ , and then decreases. The temperature coefficient of intrinsic coercivity decreases with the Fe content lowering, which should result from that reducing Fe can increase both the Curie temperature and anisotropy field, similar results were obtained by Chen et al. [8] and Guo et al. [9]. Further research [10] shows that the  $z$  value in Sm(CoFeCuZr)<sub>z</sub> magnets has a great effect on the temperature coefficient of intrinsic coercivity. In the range of  $z = 7.0$ – $8.5$ , the lower the  $z$  value is, the lower the temperature coefficient of intrinsic coercivity, and a temperature coefficient of intrinsic coercivity as low as  $-0.03$  %·°C<sup>-1</sup> can be achieved

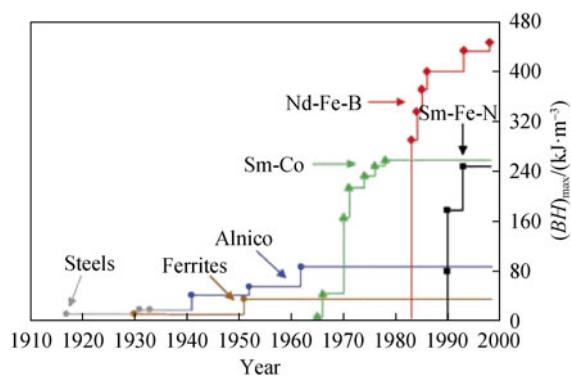


**Fig. 1** Development in energy density  $(BH)_{\max}$  at room temperature of hard magnetic materials in twentieth century [2]

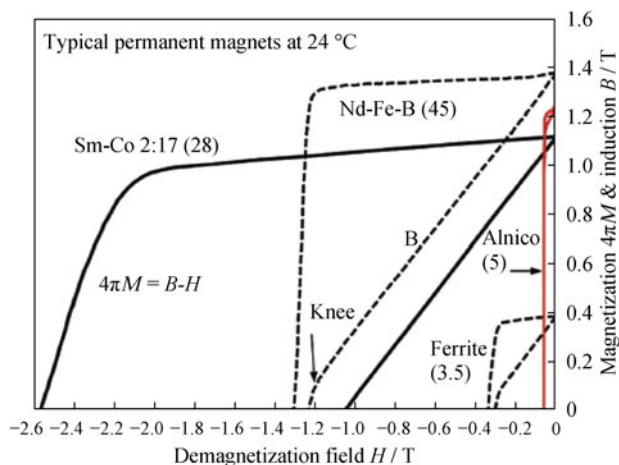


**Fig. 2** Demagnetization curves for four major permanent magnets [2]

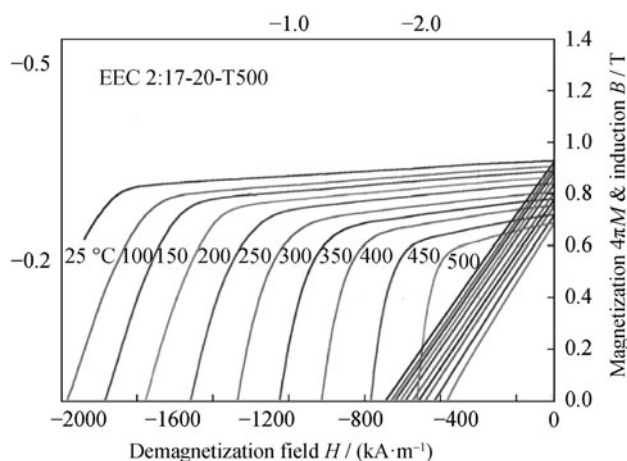


**Fig. 3** Typical demagnetization curves at various temperatures for EEC [12]

when the ratio  $z = 7.0$ , similar results were obtained by Kim [11].

Moreover, it was found that the coercivity of the magnets was closely related to heat treatment. The solution-treated temperature is essentially important for obtaining 1:7 H single phase at high temperature. And the quenching temperature during aging process has great influences on the magnetic properties of 2:17 type high temperature SmCo magnets.

Figure 3 shows the demagnetization curves of 2:17 type high temperature permanent magnets made by Electron Energy Corporation. It can be seen that the magnets have a linear  $B-H$  curve at 500 °C, which shows the magnets are suitable for high temperature applications [12].

### 2.1.2 Microstructure and microchemistry

Similar as the traditional 2:17 type SmCo magnets, 2:17 type SmCo high temperature permanent magnets possess a microstructure of cellular structure, which is composed of 2:17 R cell phase, 1:5 cell boundary phase, and Z platelet phase, as shown by Fig. 4 [7, 10]. Further analysis shows that the 2:17 R cell phase mainly consists of  $\text{Sm}_2(\text{Co}, \text{Fe})_{17}$  with  $\text{Th}_2\text{Zn}_{17}$ -type structure; the 1:5 cell phase is primarily composed of  $\text{Sm}(\text{Co}, \text{Cu})_5$  with  $\text{CaCu}_5$ -type structure, and Z phase is  $\text{Zr}(\text{Co}, \text{Fe})_3$  with the  $\text{Be}_3\text{Nb}$  structure [13]. The difference between the 2:17 type SmCo high temperature magnets and traditional 2:17 type SmCo magnets is the cell size, it can be seen in Fig. 4 that with the decrease of  $z$  value, the average cell size becomes smaller, since high Sm content (e.g. low ratio  $z$ ) would result in the formation of more  $\text{Sm}(\text{Co}, \text{Cu})_5$  cell boundary phase [10]. All the samples with lower ratio  $z$  have lower temperature coefficients of coercivity than those with higher ratio  $z$ . Therefore, it was concluded by Liu et al. [10] that smaller cell size is critical

for a better temperature dependence of coercivity. Three-dimensional atom probe (3DAP) investigation of the microchemistry of the magnets shows that during the slow cooling from 820 to 520 °C, the Cu concentration in the 1:5 phase increases, having a wider concentration profile than that of Sm at cell boundary phase (Fig. 5), which explains the substantial increase in coercivity during the slow cooling process [13]. Further analysis shows that the Cu gradient in the 1:5 cell boundary phase is essentially important for the enhancement of the coercivity [14].

### 2.1.3 Domain structure and coercivity mechanism

The formation of high coercivity in 2:17 type SmCo high temperature permanent magnets has attracted much interest in recent years. And many efforts have been devoted to investigate the domain structure and coercivity mechanism. Research shows that the fine domain structure is essential for 2:17 type SmCo high temperature permanent magnets. As shown in Fig. 6, in optimally processed high temperature 2:17 type magnets with the composition of  $\text{Sm}(\text{Co}_{0.784}\text{Fe}_{0.100}\text{Cu}_{0.088}\text{Zr}_{0.028})_{7.19}$ , the typical domain width is less than 1  $\mu\text{m}$ . While for the 2:17 type magnets quenching from the aging temperature of 850 °C, the domain structure is coarse (the width of  $\sim 10 \mu\text{m}$ ), and the coercivity is small ( $< 0.1 \text{ T}$ ). It is thought the fine domain structure can be considered as interaction domains [5].

Also, it was found that the domain structure of the magnets with abnormal temperature dependence of coercivity shows more like the strip domain, while the domain structure becomes narrower and shows more additional domains in the magnets with normal temperature dependence of coercivity, see Fig. 7 [15]. The difference of the domain structure can be attributed to whether the Cu is homogeneous in the 1:5 cell boundary phase, and this will lead to different domain wall pinning and different temperature dependence of coercivity in the magnets according to the noncontinuous domain wall pinning model. As the Cu is nearly homogeneous in the 1:5 cell boundary phase, the domain wall should be pinned near the interface between the 2:17 cell phase and 1:5 cell boundary phase, and the coercivity shows abnormal temperature dependence. On the contrary, the domain wall should be pinned into the 1:5 cell boundary phase, where a gradient of Cu content exists, leading to the normal temperature of coercivity. It can be deduced that the domain structure is related to the distribution of Cu in the 1:5 cell boundary phase.

Now it is well accepted that the large coercivity of 2:17 type permanent magnets is due to pinning of the domain walls at the 1:5 cell boundaries. For the process leading to the formation of the strong pinning barrier, Xiong et al. [13] point that the increase of Cu concentration in the 1:5 cell boundary phase can explain the substantial increase

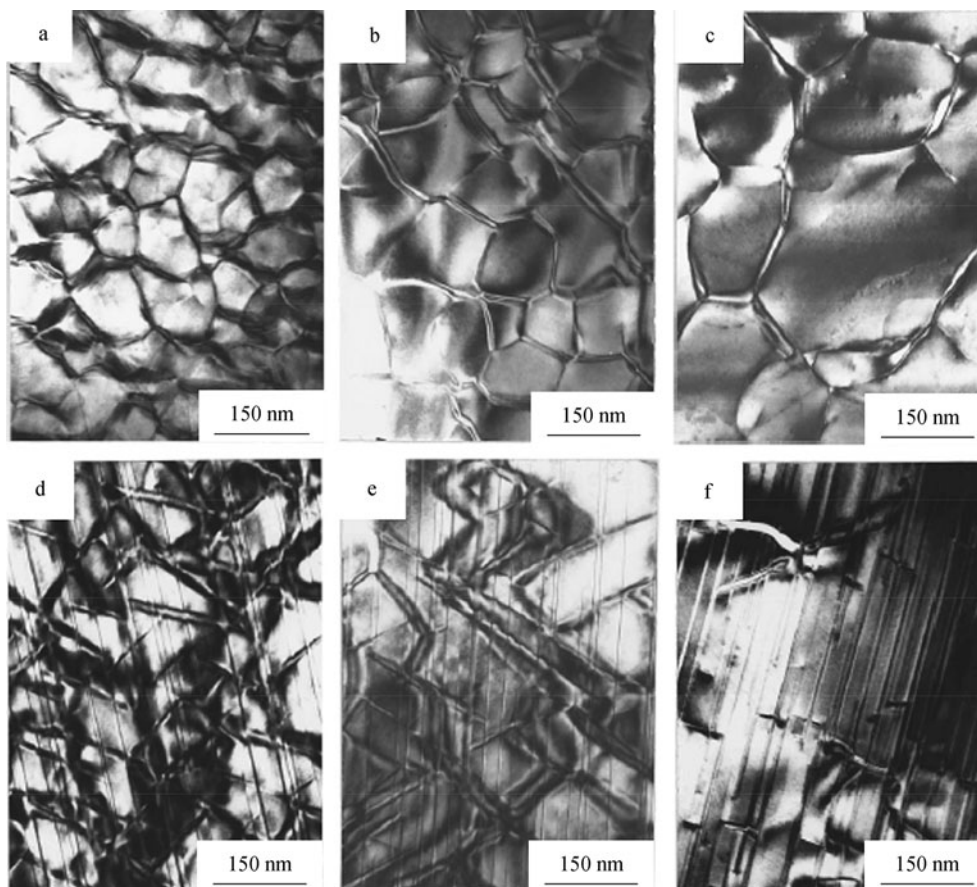


**Fig. 4** TEM images showing cellular microstructure: **a**  $z = 7.0$ , **b**  $z = 8.5$ , **c**  $z = 9.1$ , and lamellar phase **d**  $z = 7.0$ , **e**  $z = 8.5$ , **f**  $z = 9.1$  of  $\text{Sm}(\text{Co}_{\text{bal}}\text{Co}_{0.08}\text{Fe}_{0.244}\text{Zr}_{0.033})_z$  magnets [10]

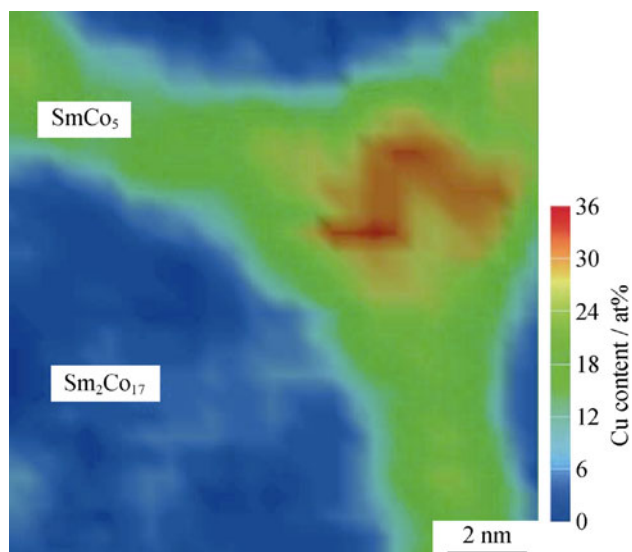


**Fig. 5** Two-dimensional Cu content map of sintered  $\text{Sm}(\text{Co}_{0.72}\text{Fe}_{0.20}\text{Cu}_{0.055}\text{Zr}_{0.025})_{7.5}$  permanent magnet quenched from 520 °C [13]

of coercivity during slow cooling process based on the atom probe results. The research of Gopalan et al. [14] by atom probe analysis revealed that the coercivity was related

to the variation in Cu concentration within the 1:5 cell boundary phase because the high-coercivity sample had a large gradient of Cu, while the low-coercivity sample revealed nearly uniform distribution of Cu within the 1:5 phase. Different from the model of the redistribution of Cu mentioned above, Goll et al. [16] think that the cell walls transform into the high-anisotropy 1:5 structure during the cooling process from 800 to 400 °C, supported by the experimental facts and micromagnetic analysis.

## 2.2 Nanocrystalline SmCo magnets

For high temperature permanent magnets, nanocrystalline SmCo magnets are another candidates and have attracted much attention, especially for the 1:7 type SmCo nanocrystalline magnets.

1:7 type nanocrystalline magnets have larger magneto-crystalline anisotropy field than the 2:17 type SmCo magnets, and the temperature coefficient of coercivity is low ( $-0.10 \text{ \%}\cdot\text{°C}^{-1}$  to  $-0.17 \text{ \%}\cdot\text{°C}^{-1}$ ) [17–19]. The magnets exhibit large coercivity at room temperature with the domain wall pinning by the nanograin boundaries [19, 20]. 1:7 type SmCo nanocrystalline magnets can be prepared directly by

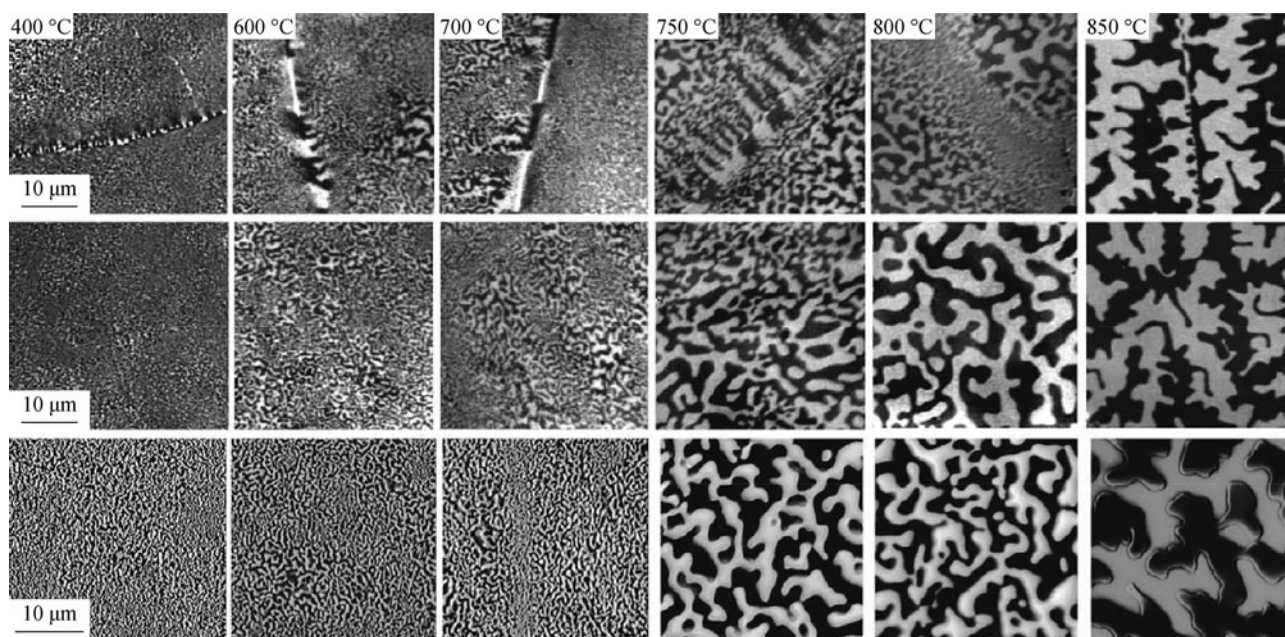


**Fig. 6** Domain structure observed by Kerr microscopy (*two top rows*) and MFM (*bottom row*) of thermally demagnetised  $\text{Sm}(\text{Co}_{0.784}\text{Fe}_{0.100}\text{Cu}_{0.088}\text{Zr}_{0.028})_{7.19}$  magnets (nominal  $c$  axis being perpendicular to imaging plane) quenched from different temperatures  $T_q$  (as indicated in the *bottom row images*) on the slow cooling ramp. Kerr images of the *first row* include in all cases a grain boundary, showing that a very specific magnetic contrast can be assigned also to the grain boundary region [5]

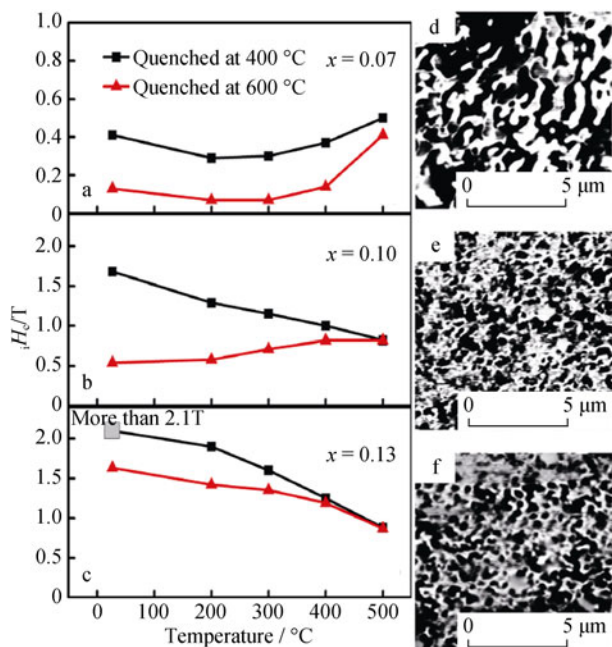


**Fig. 7** Coercivity at different temperatures for  $\text{Sm}(\text{Co}_{\text{bal}}\text{Fe}_{0.1}\text{Cu}_x\text{Zr}_{0.033})_{6.9}$  (**a**  $x = 0.07$ , **b**  $x = 0.10$ , and **c**  $x = 0.13$ ) magnets quenched at 400 and 600 °C, respectively, in the aging process and the domain structure of magnets quenched from  $T_q = 400$  °C in aging process: **d**  $x = 0.07$ , **e**  $x = 0.10$ , and **f**  $x = 0.13$  [15]

melt spinning, mechanical ball milling, or crystallization of the amorphous precursor. And 1:7 type SmCo nanocrystalline bulk magnets can be prepared by spark plasma sintering the

ball-milled amorphous powder [19, 21]. Using this method, other type of nanocrystalline bulk magnets, including  $\text{SmCo}_3$ ,  $\text{SmCo}_5$ ,  $\text{Sm}_5\text{Co}_{19}$ ,  $\text{Sm}_2\text{Co}_{17}$ , can also be prepared [22–25].

One of the main problems need to be solved is that the nanocrystalline SmCo magnets are isotropic, and it was a big challenge to prepare anisotropic nanocrystalline SmCo magnets. Hot press plus hot deformation [26, 27], surfactant-assisted ball milling plus spark plasma sintering [28], and directional annealing [29] were used to produce anisotropic nanocrystalline magnets, and a certain degree of texture can be obtained. For the hot press plus hot deformation method, increase of height reduction to 90 % leads to the formation of platelet shape grains, perpendicular to the press direction; correspondingly  $c$  axis crystallographic texture, and magnetic anisotropy were developed in the deformed magnets [26]. By combining surfactant-assisted ball milling and spark plasma sintering, a crystallographic [001] textured magnet with the average grain size of  $\sim 38$  nm and enhanced remanence ratio of 0.80 was obtained (Fig. 8) [28]. Directional annealing can produce strong (006) in-plane texture in  $\text{Sm}_{12}\text{Co}_{88}$  and  $(\text{Sm}_{12}\text{Co}_{88})_{99}\text{Nb}_1$  alloys and the anisotropy was corroborated by magnetic measurements (magnetic texture 20 %–53 %). However, the texture degree induced by these methods is not high enough and need further research.

### 2.3 Nanocomposite SmCo magnets

Nanocomposite magnets are a kind of magnets composed of hard magnetic phase that provides high coercivity and

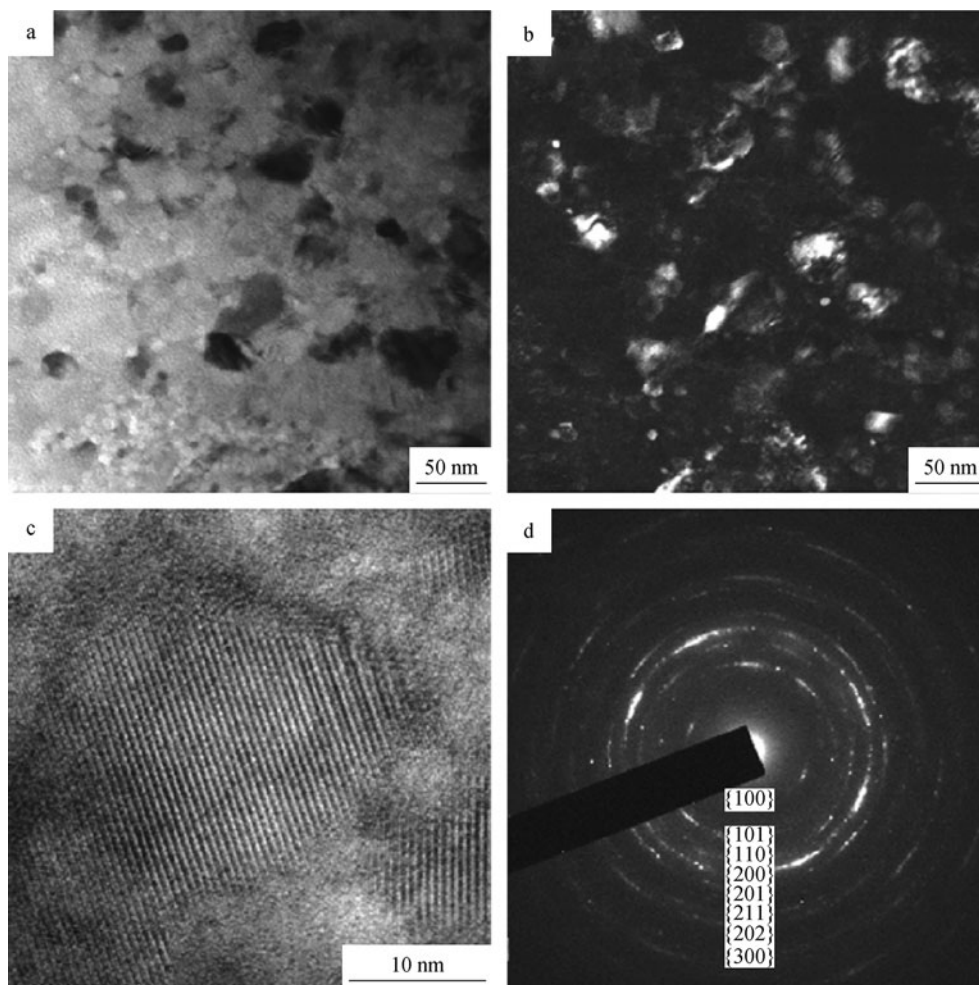


**Fig. 8** TEM images of the as-sintered bulk  $\text{SmCo}_{6.6}\text{Ti}_{0.4}$  magnets: **a** BF image, **b** DF image, **c** HRTEM image, and **d** corresponding SAED pattern. Hexagonal  $\text{TbCu}_7$ -type crystal structure being indexed by *ring pattern*. Magnets consisting of oriented nanograins with an average grain size of  $\sim 38$  nm [28]

soft magnetic phase that provides high magnetization which is potential to be the next generation of permanent magnets with very high energy product [30–32]. But making nanocomposite magnets with high performance is challenging because the grains in a successful nanocomposite magnets must be small (10 nm or less), have the right crystal structure, have aligned magnetic directions, and be tightly packed, at the same time the magnets should not react with oxygen [1].

Many efforts were devoted to produce nanocomposite magnets by using methods of reductive annealing of oxide nanoparticles [33], melt spinning [34], ball-milling plus warm compaction [35–37], ball milling plus annealing [38], mechanical milling, and consolidation [39]. By using a ball-milling plus warm compaction route, bulk  $\text{SmCo}_5/\alpha\text{-Fe}(\text{Co})$  nanocomposite magnets with enhanced energy density and thermal stability were produced [35–37]. Up to 30 % of the Fe soft magnetic phase was added to the composites with grain size  $< 20$  nm distributed homogeneously in the matrix

of the  $\text{SmCo}_5$  hard magnetic phase. It was observed that the microstructure does not change with temperature up to 500 °C. Energy products above  $88 \text{ kJ}\cdot\text{m}^{-3}$  are obtained at 300 °C in fully dense bulk  $\text{SmCo}_5/\text{Fe}$  nanocomposite magnets, which are 65 % higher than that of a single-phase counterpart at the same temperature [35].

It should be noted that most of the nanocomposite magnets prepared are magnetically isotropic which results in much lower energy product than expected. Many researches are focused on the preparation of anisotropic nanoparticles, including using chemical methods, physical methods (cluster deposition), and surfactant-assisted ball milling, which was reviewed in the Ref. [40]. It was reported that anisotropic nanocomposite magnets were prepared by hot press plus hot deformation, and surfactant-assisted ball milling plus spark plasma sintering [41, 42]. For the  $\text{SmCo}_5/\alpha\text{-Fe}$  nanocomposite prepared by hot compaction and hot deformation [42], crystal structure analysis shows that the magnets exhibit a strong *c* axis crystallographic texture of the

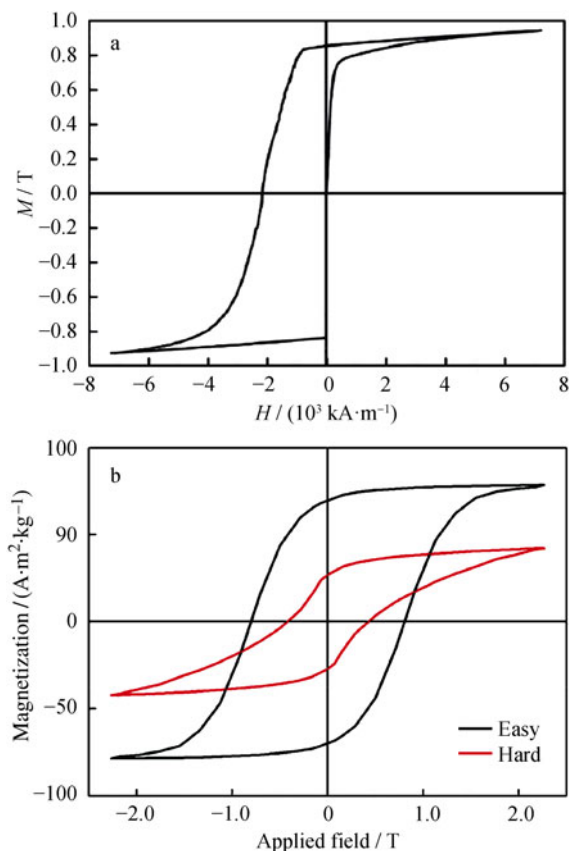


**Fig. 9** Hysteresis loop of hot deformed bulk anisotropic  $\text{SmCo}_5/\alpha\text{-Fe}$  nanocomposite magnet with 10 vol%  $\alpha\text{-Fe}$  content **a** [42]. Hysteresis loops of bulk anisotropic  $\text{SmCo}_5/\alpha\text{-Fe}$  nanocomposite magnets with 5 wt%  $\alpha\text{-Fe}$  content **b** [41]

$\text{SmCo}_5$  phase, however, the texture weakens gradually as the  $\alpha\text{-Fe}$  content increases. Microstructure observation also shows that there are many  $\text{SmCo}_5$  equiaxial grains even after hot deformation in the magnets with 15 vol%  $\alpha\text{-Fe}$ . As shown in Fig. 9a, the hot deformed bulk anisotropic  $\text{SmCo}_5/\alpha\text{-Fe}$  nanocomposite magnet with 10 vol%  $\alpha\text{-Fe}$  content exhibits the magnetic properties  $M_r$  of 0.86 T,  $H_{ci}$  of 2,128  $\text{kA}\cdot\text{m}^{-1}$ , and  $(BH)_{\max}$  of 145.68  $\text{kJ}\cdot\text{m}^{-3}$ . Anisotropic nanocomposite magnets were prepared by surfactant-assisted ball milling and spark plasma sintering. As shown in Fig. 9b, crystal structure analysis shows that all the magnets exhibit noticeable  $c$  axis crystallographic texture of  $\text{SmCo}_5$  phase. The  $\text{SmCo}_5/\alpha\text{-Fe}$  magnet with 5 wt%  $\alpha\text{-Fe}$  possesses  $M_{2.3T}$  of 78.68  $\text{A}\cdot\text{m}^2\cdot\text{kg}^{-1}$ ,  $M_r$  of 70.03  $\text{A}\cdot\text{m}^2\cdot\text{kg}^{-1}$ , and  $H_{ci}$  of 639  $\text{kA}\cdot\text{m}^{-1}$  (Fig. 9b) [41].

### 3 Oxidation protection of SmCo magnets

During the operation of high temperature permanent magnets, undesirable oxidation at high temperature is a major issue for potential applications [43–47]. Figure 10 shows

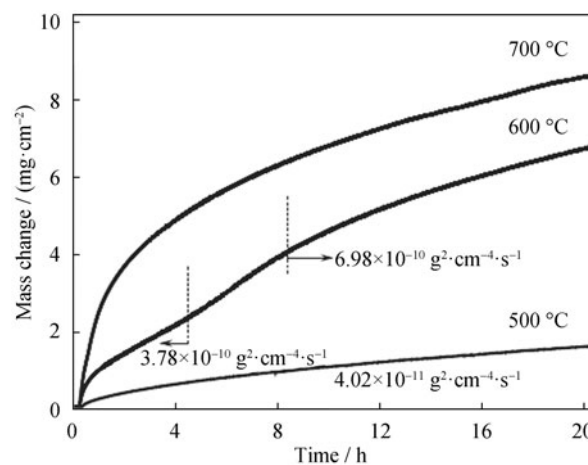


**Fig. 10** Isothermal oxidation curves of  $\text{Sm}(\text{Co}_{0.95}\text{Fe}_{0.05})_{7.5}$  alloy in air for 20 h at 500, 600, and 700 °C [46]

the isothermal oxidation curves of the  $\text{Sm}(\text{Co}_{\text{bal}}\text{Fe}_{0.22}\text{Cu}_{0.08}\text{Zr}_{0.02})_{7.5}$  alloy in air at 500–700 °C; it can be seen that the magnets oxidize at high temperature, and the oxidation becomes serious at higher temperature. Alloying [48, 49] and surface modifications [50, 51], such as Ag and Ni–S platings, were applied to improve the oxidation resistance of SmCo permanent magnets at high temperatures.

#### 3.1 Alloying

It was found that alloying Si in SmCo magnets can drastically improve their oxidation resistance, both for the 2:17 type SmCo magnets and nanocrystalline SmCo alloys [48, 49]. It can be seen from Fig. 11a–c that after oxidation at 500 °C for 500 h, the magnets with Si addition has a much thinner internal oxidation layer (IOL) than that without Si addition. And the loss of energy product with Si addition is 5.6 %, much less than that without Si addition, as shown in Fig. 11d. Further analysis shows that the formation of  $\text{SiO}_2$  oxide in the IOL plays an important role in reducing the oxidation rate and oxygen diffusion coefficient, which leads to the enhancement of inherent oxidation resistance of  $\text{SmCo}_{6.1}\text{Si}_{0.9}$  nanocrystalline magnet [48]. It should be noted that nonmagnetic element Si addition can improve the oxidation resistance of SmCo magnets, but result in the deterioration of the magnetic properties of the magnets.

#### 3.2 Surface modification

Research shows that surface modification does little effect to the magnetic properties of the magnets and can protect the magnets from oxidation effectively. As shown in Fig. 12 [50], compared with the magnets without Ni coating, the oxidation resistance of the magnets with Ni coating improves a lot. Uncoated magnets with the size of

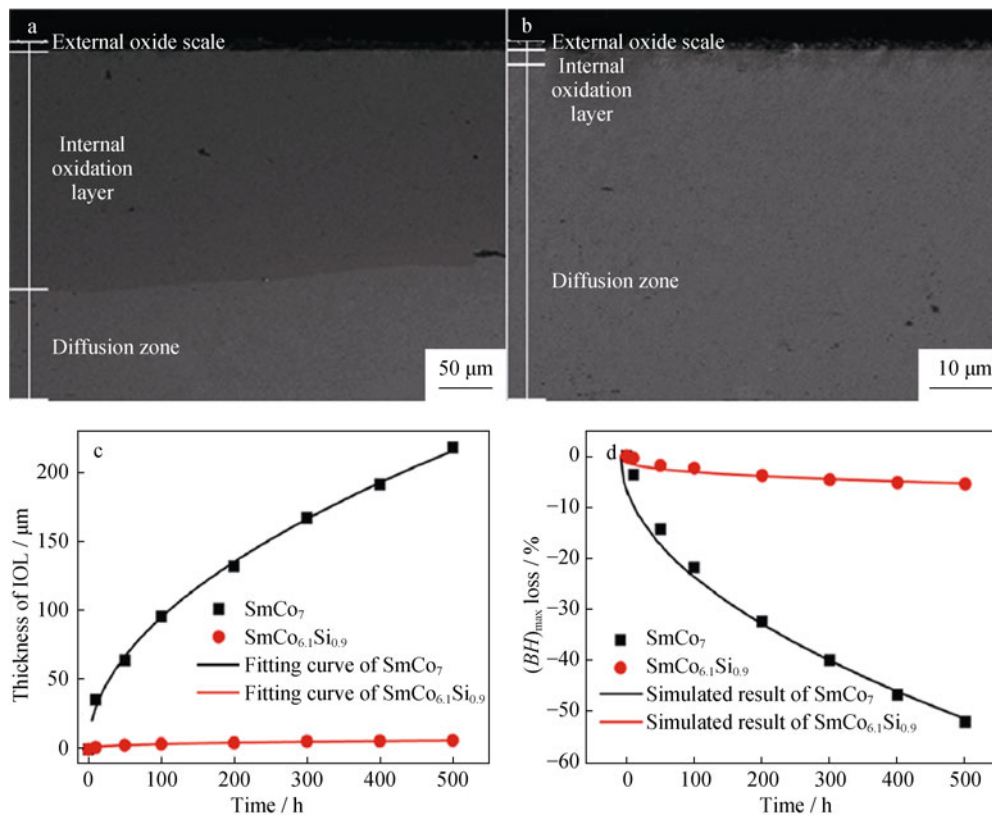


**Fig. 11** Cross-section backscattered electron images of **a**  $\text{SmCo}_7$  and **b**  $\text{SmCo}_{6.1}\text{Si}_{0.9}$  nanocrystalline magnets at 500 °C for 500 h, and dependences of thickness of internal oxidation layer (IOL) **c** and maximum energy product loss **d** for both the  $\text{SmCo}_7$  and  $\text{SmCo}_{6.1}\text{Si}_{0.9}$  nanocrystalline magnets on oxidation time at 500 °C [48]

$\phi$  10 mm  $\times$  10 mm treated at 500 °C for 500 h lost 40.8 %  $(BH)_{\text{max}}$  when remeasured at room temperature, and lost 39.1 %  $(BH)_{\text{max}}$  when measured in situ at 500 °C. While the Ni-coated magnets just lost 4.0 %  $(BH)_{\text{max}}$  and 1.2 %  $(BH)_{\text{max}}$ , respectively. And the good thermal stability of Ni-coated magnets at 500 °C can be attributed to that the Ni coating can isolate oxygen invasion and hinder Sm volatilization. Also, research reveals that at different operation temperatures, different types of coating have the best performance. For instance, the research of Pragnell et al. [52] shows that a diffused Pt coating and a paint-like overlay coating, containing Ti and Mg oxides, performed best at both 450 and 550 °C. Sputtered  $\text{SiO}_2$  was effective at 450 °C, but less so at 550 °C. Additionally, an alumina-based overlay coating was effective at 550 °C but less so at 450 °C.

#### 4 Concluding remarks and outlook

The 2:17 type SmCo magnets are now available for application at 500 °C or higher in the field of aeronautics and space limited by the cost. If the cost of the magnets can be lower, then the application will spread rapidly into the

field of new energy, such as in electronic cars and wind turbines. The magnetic performance of the magnets is sensitive to the composition and heat treatment. Compared with traditional 2:17 type SmCo magnets, the 2:17 type SmCo high temperature magnets have less Fe, higher Sm, a cellular structure with smaller size, and a much finer domain structure. The enhancement of coercivity of the magnets during the slow cooling process mainly correlates with the Cu concentration and gradient in the 1:5 phase, or the increase of anisotropy of the 1:5 phase.

Both the nanocrystalline SmCo magnets and nanocomposite SmCo magnets are potential for high temperature applications. The main problem of these two kinds of magnets is that the magnetic performance of the magnets is relatively low because it is hard to obtain high texture degree in the magnets. Many efforts have been devoted to prepare anisotropic magnets, and magnets with a certain degree texture have been produced by methods of hot compaction plus hot deformation, and surfactant-assisted ball milling plus spark plasma sintering, and directional annealing, etc. However, the preparations of anisotropic bulk nanocrystalline SmCo magnets and nanocomposite SmCo magnets with high texture degree are still big challenges and need further research. If this problem can be solved, the nanocrystalline



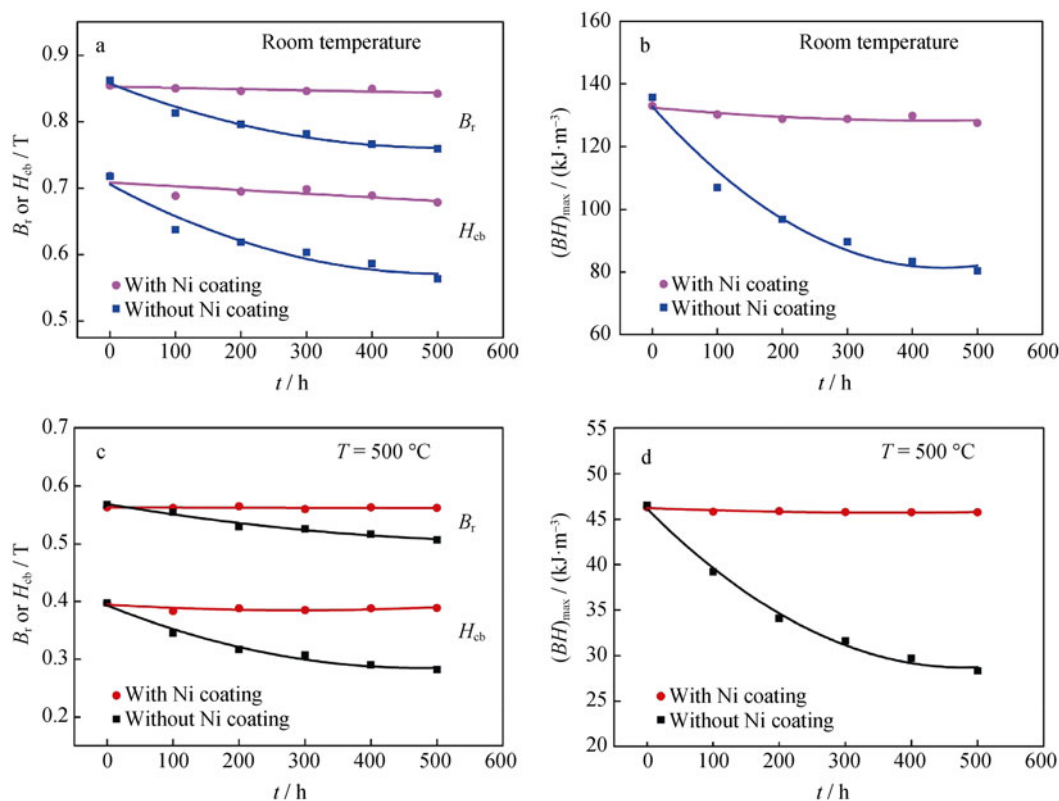


**Fig. 12** Magnetic properties of  $\text{Sm}(\text{Co}_{0.767}\text{Fe}_{0.1}\text{Cu}_{0.1}\text{Zr}_{0.033})_{6.93}$  magnets oxidized at  $500\text{ }^{\circ}\text{C}$ : **a**  $B_r$  and  $H_{cb}$  at room temperature, **b**  $(BH)_{\max}$  at room temperature, **c**  $B_r$  and  $H_{cb}$  at  $500\text{ }^{\circ}\text{C}$ , and **d**  $(BH)_{\max}$  at  $500\text{ }^{\circ}\text{C}$  [50]

SmCo magnets and nanocomposite SmCo magnets may surpass the 2:17 type SmCo magnets and become the new generation high temperature permanent magnets. And the improvement of the magnetic properties will speed the applications in the market.

During the operation of high temperature permanent magnets, undesirable oxidation at high temperatures is a major issue for potential applications. Alloying nonmagnetic element Si can effectively improve the oxidation resistance of SmCo magnets, but deteriorate the magnetic properties. Surface modification is an effective way to protect the SmCo magnets from oxidation and has little effect on the magnetic properties at the same time. For instance, Ni-coated magnets show much better stability at  $500\text{ }^{\circ}\text{C}$  than uncoated magnets. Also, research reveals that at different operation temperatures, different types of coating have the best performance.

For the high temperature permanent magnetic materials, a new research direction may be the rare-earth-free magnetic materials which do not rely on the limited supply of the rare earth metals and cost less. Further researches are needed to bring the new rare-earth-free magnetic materials for high temperature applications, and computation methods of combinational materials science may be helpful for the progress.

**Acknowledgments** This study was financially supported by the National Natural Science Foundation of China (Nos. 51071010 and 50925101), and the Innovation Foundation of Beihang University for Ph.D. Graduates.

## References

- [1] Jones N. The pull of stronger magnets. *Nature*. 2011;472:22.
- [2] Gutfleisch O, Willard MA, Bruck E, Chen CH, Sankar SG, Liu JP. Magnetic materials and devices for the 21st century: stronger, lighter, and more energy efficient. *Adv Mater*. 2011;23(7):821.
- [3] Coey JMD. Hard magnetic materials: a perspective. *IEEE Trans Magn*. 2011;47(21):4671.
- [4] Fingers RT, Rubertus CS. Application of high temperature magnetic materials. *IEEE Trans Magn*. 2000;36(5):3373.
- [5] Gutfleisch O, Müller KH, Khlopkov K, Wolf M, Yan A, Schäfer R, Gemming T, Schultz L. Evolution of magnetic domain structures and coercivity in high-performance SmCo 2:17-type permanent magnets. *Acta Mater*. 2006;54(4):997.
- [6] Provenza AJ, Montague GT, Jansen MJ, Palazzolo AB, Jansen RH. High temperature characterization of a radial magnetic bearing for turbomachinery. *J Eng Gas Turbines Power*. 2005;127(2):437.
- [7] Liu JF, Ding Y, Hadjipanayis GC. Effect of iron on the high temperature magnetic properties and microstructure of  $\text{Sm}(\text{Co}, \text{Fe}, \text{Cu}, \text{Zr})_2$  permanent magnets. *J Appl Phys*. 1999;85(3):1670.
- [8] Chen CH, Walmer MS, Walmer MH, Liu S, Kuhl E, Simon G.  $\text{Sm}_2(\text{Co}, \text{Fe}, \text{Cu}, \text{Zr})_{17}$  magnets for use at temperature  $400\text{ }^{\circ}\text{C}$ . *J Appl Phys*. 1998;83(11):6706.

- [9] Guo ZH, Pan W, Li W. Sm(Co, Fe, Cu, Zr)<sub>z</sub> sintered magnets with a maximum operating temperature of 500°C. *J Magn Magn Mater*. 2006;303:e396.
- [10] Liu JF, Zhang Y, Dimitrov D, Hadjipanayis GC. Microstructure and high temperature magnetic properties of Sm(Co, Cu, Fe, Zr)<sub>z</sub> (z = 6.7–9.1) permanent magnets. *J Appl Phys*. 1999;85(5):2800.
- [11] Kim AS. High temperature stability of SmTM magnets. *J Appl Phys*. 1998;83(11):6715.
- [12] Liu JF, Walmer MH. Thermal stability and performance data for SmCo 2:17 high-temperature magnets on PPM focusing structures. *IEEE Trans Electron Devices*. 2005;52(5):899.
- [13] Xiong XY, Ohkubo T, Koyama T, Ohashi K, Tawara Y, Hono K. The microstructure of sintered Sm(Co<sub>0.72</sub>Fe<sub>0.20</sub>Cu<sub>0.05</sub>Zr<sub>0.025</sub>)<sub>7.5</sub> permanent magnet studied by atom probe. *Acta Mater*. 2004;52(3):737.
- [14] Gopalan R, Hono K, Yan A, Gutfleisch O. Direct evidence for Cu concentration variation and its correlation to coercivity in Sm(Co<sub>0.74</sub>Fe<sub>0.1</sub>Cu<sub>0.12</sub>Zr<sub>0.04</sub>)<sub>7.4</sub> ribbons. *Scripta Mater*. 2009;60:764.
- [15] Wang GJ, Jiang CB. The coercivity and domain structure of Sm(Co<sub>0.9a</sub>Fe<sub>0.1</sub>Cu<sub>x</sub>Zr<sub>0.033</sub>)<sub>6.9</sub> (x = 0.07, 0.10, 0.13) high temperature permanent magnets. *J Appl Phys*. 2012;112(3):033909.
- [16] Goll D, Stadelmaier HH, Kronmüller H. Samarium–cobalt 2:17 magnets: analysis of the coercive field of Sm<sub>2</sub>(CoFeCuZr)<sub>17</sub> high-temperature permanent magnets. *Scripta Mater*. 2010;63(2):243.
- [17] Huang MQ, Wallace WE, McHenry M. Structure and magnetic properties of SmCo<sub>(7-x)</sub>Zr<sub>x</sub> (x = 0–0.8). *J Appl Phys*. 1998;83(11):6718.
- [18] Luo J, Liang JK, Guo YQ, Liu QL, Yang LT, Liu FS, Rao GH. Crystal structure and magnetic properties of SmCo<sub>5.85</sub>Si<sub>0.90</sub> compound. *Appl Phys Lett*. 2004;84(16):3094.
- [19] Yue M, Zhang JX, Zhang DT, Pan LJ, Liu XB, Altounian Z. Structure and magnetic properties of bulk nanocrystalline SmCo<sub>6.6</sub>Nb<sub>0.4</sub> permanent magnets. *Appl Phys Lett*. 2007;90(24):242506.
- [20] Jiang CB, Venkatesan M, Gallagher K, Coey JMD. Magnetic and structural properties of SmCo<sub>(7-x)</sub>Ti<sub>x</sub> magnets. *J Magn Magn Mater*. 2001;236:49.
- [21] Zhang ZX, Song XY, Xu WW, Seyring M, Rettenmayr M. Crystal structure and magnetic performance of single-phase nanocrystalline SmCo<sub>7</sub> alloy. *Scripta Mater*. 2010;62(8):594.
- [22] Lu N, Song X, Zhang J. Crystal structure and magnetic properties of ultrafine nanocrystalline SmCo<sub>3</sub> compound. *Nanotechnology*. 2010;21(11):115708.
- [23] Zhang Z, Song X, Qiao Y, Xu W, Zhang J, Seyring M, Rettenmayr M. A nanocrystalline Sm-Co compound for high-temperature permanent magnets. *Nanoscale*. 2013;5(6):2279.
- [24] Xu G, Yang JJ, Zhang DT, Liu WQ, Yue M, Zhang JX. Structure and magnetic properties of bulk nanocrystalline SmCo<sub>5</sub> sintered magnets. *Chin J Nonferrous Metals*. 2009;19(7):1305.
- [25] Song X, Lu N, Seyring M, Rettenmayr M, Xu W, Zhang Z, Zhang JX. Abnormal crystal structure stability of nanocrystalline Sm<sub>2</sub>Co<sub>17</sub> permanent magnet. *Appl Phys Lett*. 2009;94(2):023102.
- [26] Yue M, Zuo JH, Liu WQ, Lv WC, Zhang DT, Zhang JX, Guo ZH, Li W. Magnetic anisotropy in bulk nanocrystalline SmCo<sub>5</sub> permanent magnet prepared by hot deformation. *J Appl Phys*. 2011;109(7):07A711.
- [27] Gabay AM, Marinescu M, Liu JF, Hadjipanayis GC. Deformation-induced texture in nanocrystalline 2:17, 1:5 and 2:7 Sm–Co magnets. *J Magn Magn Mater*. 2009;321(19):3318.
- [28] An SZ, Zheng L, Zhang TL, Jiang CB. Bulk anisotropic nanocrystalline SmCo<sub>6.6</sub>Ti<sub>0.4</sub> permanent magnets. *Scripta Mater*. 2013;68(6):432.
- [29] Jayaraman TV, Shield JE. Directional annealing studies on rapidly solidified Sm–Co–Nb–C alloys. *Acta Mater*. 2012;60(3):1184.
- [30] Kneller EF, Hawig R. The exchange-spring magnet: a new material principle for permanent magnets. *IEEE Trans Magn*. 1991;27(4):3588.
- [31] Skomski R, Coey JMD. Giant energy product in nanostructured two-phase magnets. *Phys Rev B*. 1993;48(21):15812.
- [32] Cui WB, Takahashi YK, Hono K. Nd<sub>2</sub>Fe<sub>14</sub>B/FeCo anisotropic nanocomposite films with a large maximum energy product. *Adv Mater*. 2012;24(48):6530.
- [33] Hou Y, Sun S, Rong C, Liu JP. SmCo<sub>5</sub>/Fe nanocomposites synthesized from reductive annealing of oxide nanoparticles. *Appl Phys Lett*. 2007;91(15):153117.
- [34] Shield JE, Ravindran VK, Aich S, Hsiao A, Lewis LH. Rapidly solidified nanocomposite SmCo<sub>7</sub>/fcc-Co permanent magnets. *Scripta Mater*. 2005;52(1):75.
- [35] Rong C, Poudyal N, Liu XB, Zhang Y, Kramer MJ, Liu JP. High temperature magnetic properties of SmCo<sub>5</sub>/α-Fe(Co) bulk nanocomposite magnets. *Appl Phys Lett*. 2012;101(15):152401.
- [36] Rong C, Zhang Y, Poudyal N, Xiong X, Kramer MJ, Liu JP. Fabrication of bulk nanocomposite magnets via severe plastic deformation and warm compaction. *Appl Phys Lett*. 2010;96(10):102513.
- [37] Zhang Y, Kramer MJ, Rong C, Liu JP. Microstructure and intergranular diffusion in exchange-coupled Sm–Co/Fe nanocomposites. *Appl Phys Lett*. 2010;97(3):032506.
- [38] Liu Z, Chen RJ, Lee D, Yan AR. Influence of milled α-Fe powders on structure and magnetic properties of Sm(Co, Zr)<sub>7</sub>/α-(Fe, Co) nanocomposite magnets made by mechanical alloying. *J Appl Phys*. 2011;109(7):07A752.
- [39] Rao NVR, Gopalan R, Raja MM, Chandrasekaran V, Chakravarthy D, Sundaresan R, Ranganathan R, Hono K. Structural and magnetic studies on spark plasma sintered SmCo<sub>5</sub>/Fe bulk nanocomposite magnets. *J Magn Magn Mater*. 2007;312(2):252.
- [40] Balamurugan B, Sellmyer DJ, Hadjipanayis GC, Skomski R. Prospects for nanoparticle-based permanent magnets. *Scripta Mater*. 2012;67(6):542.
- [41] Hu DW, Yue M, Zuo JH, Pan R, Zhang DT, Liu WQ, Guo ZH, Li W. Structure and magnetic properties of bulk anisotropic SmCo<sub>5</sub>/α-Fe nanocomposite permanent magnets prepared via a bottom up approach. *J Alloys Compd*. 2012;538:173.
- [42] Liu WQ, Zuo JH, Yue M, Cui ZZ, Zhang DT, Zhang JX, Zhang PY, Ge HL, Guo ZH, Li W. Structure and magnetic properties of bulk anisotropic SmCo<sub>5</sub>/α-Fe nanocomposite permanent magnets with different α-Fe content. *J Appl Phys*. 2011;109(7):07A741.
- [43] Pragnell WM, Evans HE, Williams AJ. The oxidation kinetics of SmCo alloys. *J Alloys Compd*. 2009;473(1–2):389.
- [44] Pragnell WM, Williams AJ, Evans HE. The oxidation morphology of SmCo alloys. *J Alloys Compd*. 2009;487(1–2):69.
- [45] Pragnell WM, Williams AJ, Evans HE. The oxidation of SmCo magnets. *J Appl Phys*. 2008;103(7):07E127.
- [46] Yang Z, Peng X, Feng Q, Guo Z, Li W, Wang F. The mechanism of high temperature oxidation of a SmCo-based magnetic alloy. *Corros Sci*. 2012;61:72.
- [47] Qadeer MI, Azhdar B, Hedenqvist MS, Savage SJ. Anomalous high temperature oxidation of Sm<sub>2</sub>(Fe, Co, Cu, Zr)<sub>17</sub> particles. *Corros Sci*. 2012;65:453.
- [48] Liu LL, Jiang CB. The improved oxidation resistance of Si-doped SmCo<sub>7</sub> nanocrystalline magnet. *Appl Phys Lett*. 2011;98(25):252504.
- [49] Liu LL, Jin TY, Jiang CB. High-temperature oxidation resistance and magnetic properties of Si-doped Sm<sub>2</sub>Co<sub>17</sub>-type magnets at 500 °C. *J Magn Magn Mater*. 2012;324(14):2310.
- [50] Wang QY, Zheng L, An SZ, Zhang TL, Jiang CB. Thermal stability of surface modified Sm<sub>2</sub>Co<sub>17</sub>-type high temperature magnets. *J Magn Magn Mater*. 2013;331:245.
- [51] Chen CH, Huang MQ, Foster JE, Monnette G, Middleton J, Higgins A, Liu S. Effect of surface modification on mechanical properties and thermal stability of Sm–Co high temperature magnetic materials. *Surf Coat Technol*. 2006;201(6):3430.
- [52] Pragnell WM, Evans HE, Williams AJ. Oxidation protection of Sm<sub>2</sub>Co<sub>17</sub>-based alloys. *J Alloys Compd*. 2012;517:92.